Journal of Solid State Chemistry 181 (2008) 3283–3286

Contents lists available at ScienceDirect

Journal of Solid State Chemistry

journal homepage: www.elsevier.com/locate/jssc

Microscopic studies of a SnO_2/α-Fe_2O_3 architectural nanocomposite using Mössbauer spectroscopic and magnetic measurements

Naoaki Hayashi [a,*], Shigetoshi Muranaka [a], Shinpei Yamamoto [b], Mikio Takano [b,1], Dong-Feng Zhang [c], Ling-Dong Sun [c], Chun-Hua Yan [c]

[a] Graduate School of Human and Environmental Studies, Kyoto University, Yoshida-nihonmatsu, Sakyo, Kyoto 606-8501, Japan
[b] Institute for Chemical Research, Kyoto University, Gokasho, Uji, Kyoto 611-0011, Japan
[c] State Key Lab of Rare Earth Materials Chemistry and Applications, & PKU-HKU Joint Lab in Rare Earth Materials and Bioinorganic Chemistry, Peking University, Beijing 100871, China

ARTICLE INFO

Article history:
Received 11 March 2008
Received in revised form
20 August 2008
Accepted 1 September 2008
Available online 18 September 2008

Keywords:
Mössbauer spectroscopy
SnO_2/α-Fe_2O_3 nanocomposite

ABSTRACT

A SnO_2/α-Fe_2O_3 architectural nanocomposite, which was evidenced as SnO_2 nanorod arrays assembled on the surface of α-Fe_2O_3 nanotubes in our previous study, was investigated microscopically by means of Mössbauer spectroscopic and magnetic measurements. It was found for the SnO_2 nanorods that Fe^{3+} ions substituted slightly to $Sn_{0.998}Fe_{0.002}O_2$. Concerning the α-Fe_2O_3 tubes, the Morin transition, which was completely suppressed in the mother, SnO_2-free α-Fe_2O_3 nanotubes, was found to be recovered locally. We speculate that it takes place in the interface area as a result of structural modification needed for the connection with the SnO_2 nanorods.

1. Introduction

As promising candidates for nanodevice construction, nanocomposites with complex structures have become a research focus in recent years. Mentioning some examples, ZnO/In_2O_3 hierarchical structures with different symmetries [1], GaP/GaP and GaP/GaAsP tree-like arrays [2], CdE (E = S, Se, and Te) heterostructures with linear and branched morphologies [3], and ZnO- and TiO_2-based nanoblocks assembled into brush-like architectures [4] have been reported. Spontaneous or designed organization of building blocks is of the greatest interest in these studies, but it should be kept in mind that the blocks themselves may be more or less modified through the organizing processes.

The magnetism of α-Fe_2O_3 is quite interesting [5]. A drastic spin flipping takes place at $T_M = 263$ K, which is called the Morin transition. In the high-temperature (high-T) phase, the atomic spins lie within the (001) plane of the hexagonal structure, while they are aligned perpendicular to the plane in the low-T phase. The high-T phase is a spin-canted weak ferromagnet, while the low-T phase is a simple antiferromagnet without any spin canting. Of special interest from the viewpoint of nanoscience is that the Morin transition can be suppressed, or the weak ferromagnetism can be preserved down to low temperatures by decreasing the particle size, for example [6]. Driven by potential physical and chemical applications and also as a challenge in morphology control approach, SnO_2 nanorods were assembled on the surface of hexagonal α-Fe_2O_3 nanotubes and their structural matching was studied as reported previously [7]. In this paper, we will report the magnetism and related microstructural aspects studied by means of Mössbauer spectroscopic and magnetic characterizations.

2. Experimental

The detailed assembling process is described elsewhere [7]. Briefly, α-Fe_2O_3 nanotubes grown along the c-axis were first synthesized by a coordination-assisted dissolution process [8], and were then dispersed in a $Sn(OH)_6^{2-}$-containing solution and converted to the SnO_2/α-Fe_2O_3 hierarchical architectures by a hydrothermal process.

The compositional analysis of the product was carried out with inductively coupled plasma (ICP, Vario EL, Elementar), and the morphology was investigated by scanning electron microscopy (SEM, DB-235 focused ion beam system). Magnetic measurements were carried out using a SQUID magnetometer (Quantum Design, MPMS2) on field cooling (FC) and also on heating after zero-field cooling (ZFC) at a magnetic field of 100 Oe in a temperature range

* Corresponding author.
E-mail address: hayashi@sou.mbox.media.kyoto-u.ac.jp (N. Hayashi).
[1] Present address: Institute for Cell-Material Integrated Sciences, Kyoto University, c/o Research Institute for Production Development, 15 Morimoto, Shimogamo, Sakyo, Kyoto 606-0805, Japan.

0022-4596/$ - see front matter Crown Copyright © 2008 Published by Elsevier Inc. All rights reserved.
doi:10.1016/j.jssc.2008.09.001

of 5–300 K. The field dependence was studied at certain fixed temperatures up to 10 kOe. Mössbauer spectra were measured in transmission geometry using ^{57}Co/Rh and Ca^{119m}SnO$_3$ as the γ-ray sources. The velocity scale and the isomer shift were determined by using α-Fe and CaSnO$_3$ as the control samples, and the resulting spectra were least-squares-fitted using the Lorentzian function.

3. Results and discussion

Fig. 1 shows a typical SEM image of the SnO$_2$/α-Fe$_2$O$_3$ architecture. It can be seen that the composites are essentially of 6-fold symmetry with secondary SnO$_2$-nanorod arrays of 10–15 nm in diameter and 70–100 nm in length. The original α-Fe$_2$O$_3$ nanotubes were 90–100 nm in outer diameter, 40–80 nm in inner diameter, and 250–400 nm in length. Based on an HRTEM characterization, the interfacial orientation relationship was determined as SnO$_2$ (101)//α-Fe$_2$O$_3$ (110) [7].

Fig. 2(a) shows the ^{57}Fe Mössbauer spectra, which consists of components characterized by the parameters listed in Table 1. At room temperature, the sextet (component II) coincides with the pattern of the high-T phase of normal α-Fe$_2$O$_3$, while the doublet, component I, was the new presence that had not been detected from the mother α-Fe$_2$O$_3$ nanotubes. This component could not be attributed to the formation of very fine, superparamagnetic α-Fe$_2$O$_3$ particles because the quadrupole splittings (QSs) of this doublet are considerably larger than expected and also because the previous TEM observations did not detect such particles anywhere in the sample, either in the SnO$_2$/α-Fe$_2$O$_3$ interface region or within the SnO$_2$ nanorods [7]. According to the report by Castro et al. on 2–30 mol% Fe-doped SnO$_2$ nanoparticles synthesized by a polymeric precursor method [9], the spectrum generally consisted of a pair of paramagnetic doublets having different QSs of ~0.7 and ~1.6–1.2 mm s^{-1}, the smaller QS-component being assigned to Fe^{3+} ions distributed in the inner part of the SnO$_2$ crystal, and the larger QS-component to Fe^{3+} ions concentrated in the surface area where the SnO$_2$ lattice was distorted as a result of the segregation of excess Fe ions beyond the solubility limit. Therefore, the portion of the former doublet decreased with increasing Fe concentration. Concerning the present case, all the Fe ions may be concluded to be dissolved in the SnO$_2$ rods homogeneously, without being segregated locally, considering the facts that the single doublet has a relatively small QS of ~0.65 mm s^{-1} and that the Fe content is so small as ~0.2 mol% as will be described later. It is very likely that the original α-Fe$_2$O$_3$ nanotubes partially dissolved and the ferric ions formed were incorporated into the growing SnO$_2$ nanorods in the hydrothermal assembling process. Fig. 2(b) shows the ^{119}Sn spectrum at room temperature, which has been assigned to the

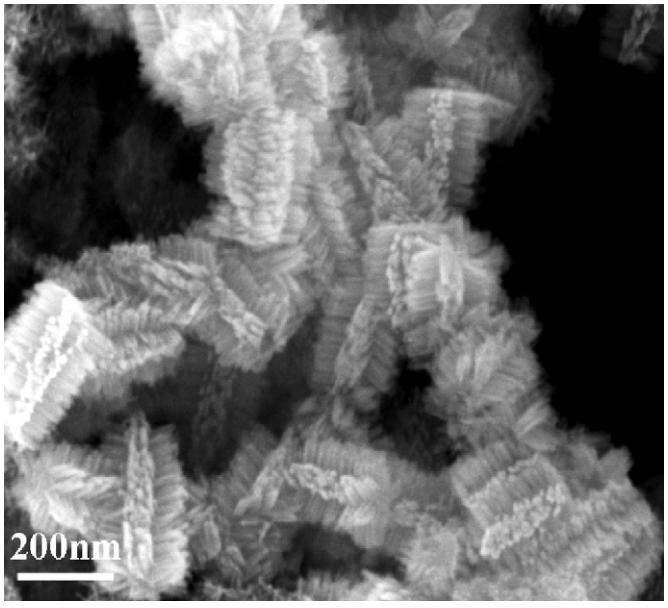

Fig. 1. SEM image of the SnO$_2$/α-Fe$_2$O$_3$ architecturral nanocomposite.

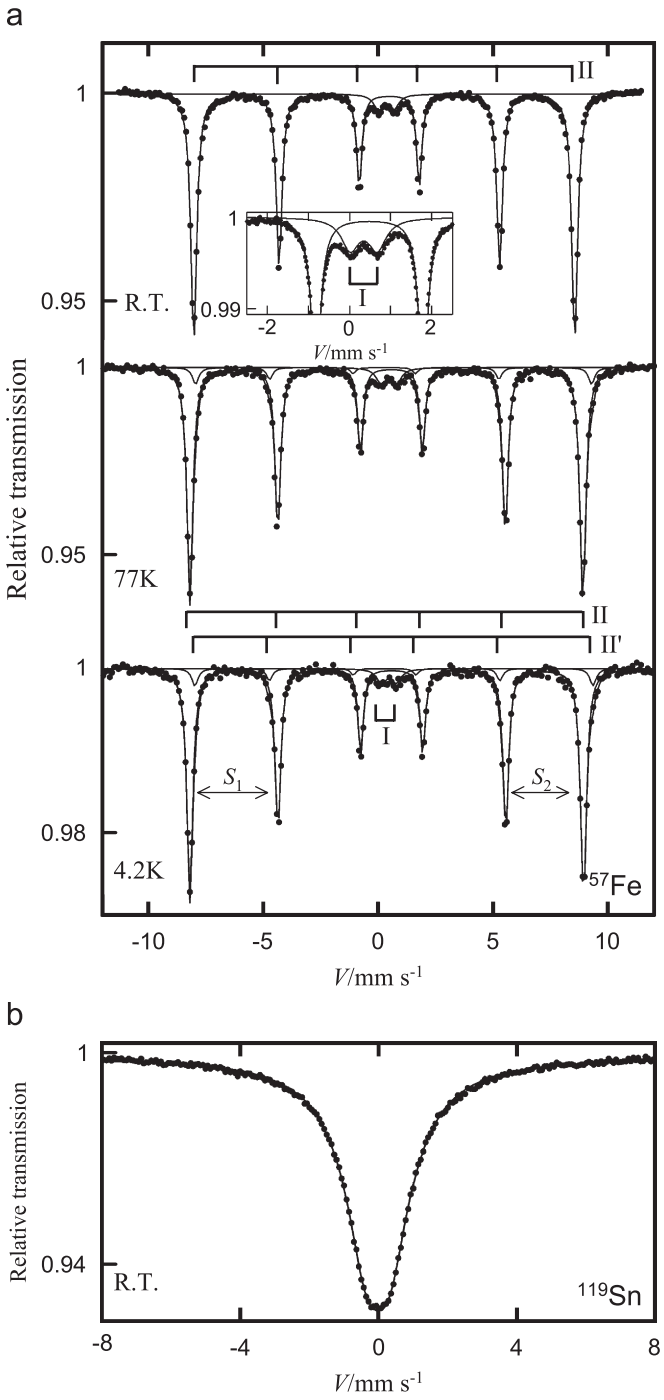

Fig. 2. (a) ^{57}Fe Mössbauer spectra of the SnO$_2$/α-Fe$_2$O$_3$ architectural nanocomosite. Inset shows the spectrum expanded in a narrow velocity range. (b) ^{119}Sn Mössbauer spectrum of the SnO$_2$/α-Fe$_2$O$_3$ architecture.

Table 1
^{57}Fe and ^{119}Sn Mössbauer parameters of SnO_2/α-Fe_2O_3

T (K)	Component	IS (mm s^{-1})	HF (kOe)	QS (mm s^{-1})	$(S_2-S_1)/2$	Γ (mm s^{-1})	Area (%)
^{57}Fe							
RT	I	0.35	–	0.66	–	0.52	4.7±0·3
	II	0.38	513	–	−0.22	0.29	95.3±0·9
77	I	0.47	–	0.67	–	0.51	5±1
	II	0.47	529	–	−0.22	0.29	88±2
	II′	0.47	534	–	0.41	0.30	7±1
4.2	I	0.47	–	0.65	–	0.52	4±1
	II	0.49	530	–	−0.22	0.29	89±2
	II′	0.48	536	–	0.41	0.30	7±1
^{119}Sn							
RT	–	−0.01	–	0.60	–	1.7	100

Note: IS: isomer shift (relative to α-Fe), HF: hyperfine interaction, QS: quadrupole splitting, $(S_2-S_1)/2$: quadrupole shift in a magnetically split pattern (see Fig. 2(a)), Γ: full-width at half-maximum of the absorption line, Area: relative area of the component.

normal tetragonal SnO_2 (see Table 1) [10]. Any influence of the partial Fe^{3+} substitution was not visible.

If we write down the total composition of the present architecture as $y(Sn_{1-x}Fe_xO_2)-(1-y)(\alpha\text{-}Fe_2O_3)$, the relationship among x, y, and the area ratios of the different components in the ^{57}Fe spectrum are given by

$$xy/\{2(1-y)+xy\} = \text{area(I)}, \quad \text{or}$$
$$(1-y)/\{2(1-y)+xy\} = \text{area(II)}. \tag{1}$$

The total Sn:Fe atomic ratio is given by

$$y(1-x)/\{xy+2(1-y)\} = [\text{Sn}]/[\text{Fe}]. \tag{2}$$

Using the ICP result of $[\text{Sn}]/[\text{Fe}] = 19.87$, we obtain

$$x = 0.002 \quad \text{and} \quad y = 0.977. \tag{3}$$

That is, the composition we deduced here is $0.977(Sn_{0.998}Fe_{0.002}O_2)-0.023(\alpha\text{-}Fe_2O_3)$. It is known that the solubility of α-Fe_2O_3 in SnO_2 is almost negligible in the thermal equilibrium state [11–13] though the real solubility can be drastically increased by using special preparative processes (see [13] for example). The present Mössbauer data suggest that the Fe content of 0.2 mol% is below the solubility limit under the preparative conditions.

Fig. 3(a) shows the temperature dependence of magnetization (M) divided by an applied field (H), M/H, for the SnO_2/α-Fe_2O_3 architecture measured at $H = 100$ Oe on cooling (FC) and on heating after zero-field cooling (ZFC). These curves are greatly separated from each other because the highest measuring temperature of 300 K was much lower than the T_N of 956 K and also because the field applied was smaller than the coercive field of ~1 kOe (see Fig. 3(b)). A small stepwise change in M due to the Morin transition was observed at ~170 and ~210 K for FC and ZFC, respectively (see the insets also). Compared in the inset for the FC data are the magnetization normalized at 300 K, $M/M_{300\,K}$, for the present SnO_2/α-Fe_2O_3 composite and that for the mother α-Fe_2O_3-nanotubes. It is clear that any anomaly due to the Morin transition is absent in the latter but it is present at ~170 K in the former.

The magnetic features of the present system can be summarized as below. Firstly, the T_M, which is ~170 K and ~210 K for FC and ZFC, respectively, is considerably lower than the normal one of ~260 K and, secondly, the ZFC and FC curves do not coincide below T_M as expected from the simple antiferromagnetic nature of the low-T phase. Thirdly, the difference of ~40 K in T_M between

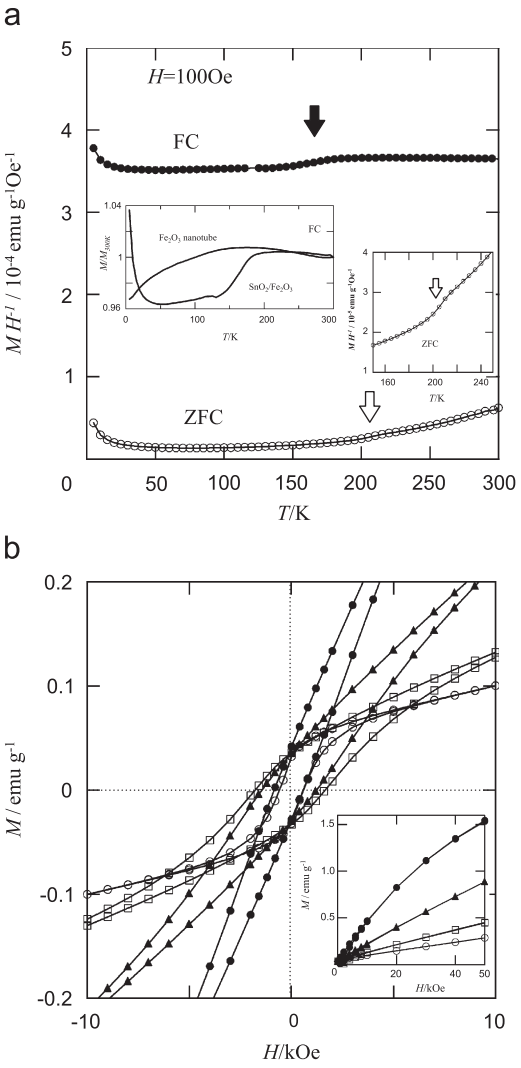

Fig. 3. (a) Temperature dependence of magnetization divided by applied field, M/H, for the SnO_2/α-Fe_2O_3 architectural nanocomposite measured on field-cooling (FC, ●) and on heating after zero-field cooling (ZFC, ○). The arrows mark the temperatures of the Morin transition, T_M. Inset for the FC data shows the temperature dependence of magnetization normalized at 300 K, $M/M_{300\,K}$, for the SnO_2/α-Fe_2O_3 architectural nanocomposite, and also that for the mother, SnO_2-free α-Fe_2O_3 nanotubes. The ZFC data in the transition region are magnified in the inset on the right. (b) M–H curves taken at 5 K (●), 20 K (▲), 77 K (□), and 300 K (○).

the FC and ZFC results is much larger than the normal thermal hysteresis of ~5 K for α-Fe_2O_3 [14]. Fourthly, the magnetization increases considerably below ~30 K, which is also unexpected from the antiferromagnetic nature of the low-T phase. In fact, however, this should be owed not to the α-Fe_2O_3 nanotubes but to the $Sn_{0.998}Fe_{0.002}O_2$ nanorods that remain paramagnetic down to 4 K as can be seen in the persistence of the pair of paramagnetic doublet in the low-temperature Mössbauer spectra (see Fig. 2(a) and Table 1).

Concerning the first feature, it is well known that the T_M of fine particles is lowered depending on their size, shape, purity, lattice strain, and lattice defect [5]. It is not clear as to why the mother nanotubes do not exhibit the Morin transition but we speculate that the thinness of the tube wall of a few tens of nm and also the lattice strain or defects are the possible origins. The second feature can be understood if the transition takes place only in a minor part of the α-Fe_2O_3 nanotubes. The hysteretic M–H curves shown in Fig. 3(b) surely manifested the persistence of weak ferromagnetic phase down to 4 K. A quantitative estimation was

done using Mössbauer spectroscopy. The high- and low-T phases can be quite easily identified because the quadrupole shift, $(S_2-S_1)/2$, is known to have different values and opposite signs as $\sim-0.2\,\mathrm{mm\,s^{-1}}$ for the former but $\sim+0.4\,\mathrm{mm\,s^{-1}}$ for the latter. The experimental spectra at 77 and 4 K in Fig. 2(a) show that the low-T phase (component II′) is a minority of only 7:90 in comparison with the high-T phase (component II) (see Table 1). Now it is clear that $7(\pm1)$ vol% of the α-Fe_2O_3-nanotubes recovered the Morin transition after the deposition of the SnO_2-nanorods. We speculate that a certain structural modification needed for the lattice matching in the interface region has led to the recovery. The large difference of $\sim$40 K in T_M between FC and ZFC, the third feature mentioned above, may also have resulted from such a specific structural feature.

By the way, Coey et al. [15] reported that Fe-doped SnO_2 thin films showed ferromagnetism with a T_C of 610 K. The Fe content was 14 mol% but it was a quarter of it that was involved in the ferromagnetism. Fitzgerald et al. [16] made a related study indicating ferromagnetism with a T_C of 360 K for a powdered sample with a nominal Fe content of 5 mol% prepared using thermal solid-state reactions. In comparison with these results, our analysis means that the SnO_2 nanorods doped with Fe up to 0.2 mol% remains paramagnetic down to 4 K.

4. Conclusion

A specific SnO_2/α-Fe_2O_3 architectural nanocomposite made of α-Fe_2O_3 nanotubes with SnO_2 nanorods grafted centripetally around them was investigated by Mössbauer spectroscopic and magnetic measurements. The composition was deduced to be $0.977(Sn_{0.998}Fe_{0.002}O_2)-0.023(\alpha\text{-}Fe_2O_3)$, that is, the SnO_2 nanorods contained $\sim$0.2% of Fe^{3+} ions. The α-Fe_2O_3 nanotubes showed the Morin transition locally, to $\sim$7% in volume. These were suggested to have resulted from chemical and structural changes taking place in the SnO_2-grafting process.

Acknowledgments

This work was partly supported by the Grants-in-Aid 17105002, 15750050, 14204070, 20750046, and 12CE2005 from the Ministry of Education, Science, Sports and Culture, Japan.

References

[1] J.Y. Lao, J.G. Wen, Z.F. Ren, Nano Lett. 2 (2002) 1287.
[2] K.A. Dick, K. Deppert, M.W. Larsson, T. Mårtensson, W. Seifert, L.R. Wallenberg, L. Samuelson, Nat. Mater. 3 (2004) 380.
[3] D.J. Milliron, S.M. Hughes, Y. Cui, L. Manna, J.B. Li, L.W. Wang, A.P. Alivisatos, Nature (London) 430 (2004) 190.
[4] H.G. Yang, H.C. Zeng, J. Am. Chem. Soc. 127 (2005) 270.
[5] R.M. Cornell, U. Schwertmann, The Iron Oxides, second ed., Wiley-VCH, Weinheim, 2003.
[6] Y. Bando, M. Kiyama, N. Yamamoto, T. Takada, T. Shinjo, H. Takaki, J. Phys. Soc. Japan 20 (1965) 2086.
[7] D.F. Zhang, L.D. Sun, C.J. Jia, Z.G. Yan, L.P. You, C.H. Yan, J. Am. Chem. Soc. 127 (2005) 13492.
[8] C.J. Jia, L.D. Sun, Z.G. Yan, L.P. You, F. Luo, X.D. Han, Y.C. Pang, Z. Zhang, C.H. Yan, Angew. Chem. Int. Ed. 44 (2005) 4328.
[9] R.H.R. Castro, P. Hidalgo, J.A.H. Coaquira, J. Bettini, D. Zanchet, D. Gouvêa, Eur. J. Inorg. Chem. 11 (2005) 2134.
[10] N.N. Greenwood, T.C. Gibb, Mössbauer Spectroscopy, Chapman & Hall, London, 1971, 371pp.
[11] J. Cassedanne, An. Acad. Bras. Cien 38 (1996) 265.
[12] G.H. Moh, Chem. Erde 33 (1974) 243.
[13] M. Takano, Y. Bando, N. Nakanishi, M. Sakai, H. Okinaka, J. Solid State Chem. 68 (1987) 153.
[14] E. Krén, B. Molnàr, E. Svàb, É. Zsoldos, Solid State Commun. 15 (1974) 1707.
[15] J.M.D. Coey, A.P. Douvalis, C.B. Fitzgerald, M. Venkatesan, Appl. Phys. Lett. 84 (2004) 1332.
[16] C.B. Fitzgerald, M. Venkatesan, A.P. Douvalis, S. Huber, J.M.D. Coey, T. Bakas, J. Appl. Phys. 95 (2004) 7390.